European Polymer Journal 46 (2010) 2042–2050

Contents lists available at ScienceDirect

European Polymer Journal

journal homepage: www.elsevier.com/locate/europolj

Response mechanism of novel polyaniline composite conductimetric pH sensors and the effects of polymer binder, surfactant and film thickness on sensor sensitivity

E. Gill [a,1], A. Arshak [a,*], K. Arshak [b,2], O. Korostynska [b,3]

[a] Department of Physics, University of Limerick, Ireland
[b] Department of Electronic and Computer Engineering, University of Limerick, Ireland

ARTICLE INFO

Article history:
Received 25 March 2010
Received in revised form 13 July 2010
Accepted 27 July 2010
Available online 16 August 2010

Keywords:
Conductimetric
pH
Sensor
Thick films
Conducting polymers

ABSTRACT

This paper reports on investigations into the response mechanism of novel polyaniline composition conductimetric pH sensors and the effects of polymer binder, surfactant and film thickness on this response. It was revealed through X-ray photoelectron spectroscopy, focussed ion beam milling and impedance spectroscopy that the response mechanism was due to the deprotonation of the polymer backbone nitrogen atoms located on the uppermost surface level of the functional material particles. The equivalent circuits for the sensing layer were modelled using the Cole–Cole model for a range of pH environments. The optimum sensing layer composition was determined to contain less than 50 wt.% polymer binder with 5 wt.% surfactant. This composition was determined by examining the effects of both binder and surfactant on the electrical characteristics and sensor response of the composite films. The thickness of the sensing layer was found to have no discernable response on the sensing characteristics of the conductimetric pH sensors.

1. Introduction

Conductimetric sensors have frequently appeared in the literature for a variety of applications, including; gas sensors [1,2], humidity sensors [3,4], and sensors to measure biologically significant molecules such as urea [5] and glucose [6,7]. One application in which conductimetric sensors cannot be commonly found is pH sensing. The principal reason for the lack of publications describing conductimetric pH sensors is the popularity and reliability of other approaches, such as the potentiometric sensor and the more common glass electrode measurement systems. While glass electrodes have been available since the early 1920's [8,9], the miniaturisation potential associated with them is quite limited due to the complicated and expensive construction required and the fragile nature of the materials involved. For a truly miniaturised pH sensor, researchers focussed on other novel approaches. The most common miniaturised sensor available today is the potentiometric sensor, which functions in a similar way to the glass electrode. However, potentiometric sensors have their draw backs, which include sensor output drift and ionic interference [10] from other species in the solution under measurement.

A conductimetric sensor, on the other hand requires only two simple fabrication steps: (1) the deposition of two identical electrodes; and (2) the deposition of the pH-sensitive layer. Once the sensor is exposed to a solution, the resistance/conductance of the sensing layer will change (pH-dependent) resulting in a simple, cost effective and reliable pH sensor. There have been several papers published describing such sensors [11,12], and recently our research group have published several papers describing several of these sensors [13–15].

* Corresponding author. Tel.: +353 61 202371; fax: +353 61 202423.
E-mail addresses: edric.gill@ul.ie (E. Gill), Arousian.Arshak@ul.ie (A. Arshak), khalil.arshak@ul.ie (K. Arshak), olga.korostynska@ul.ie (O. Korostynska).
[1] Tel.: +353 61 202371; fax: +353 61 202423.
[2] Tel.: +353 61 202267; fax: +353 61 338176.
[3] Tel.: +353 61 234254; fax: +353 61 338176.

0014-3057/$ - see front matter © 2010 Elsevier Ltd. All rights reserved.
doi:10.1016/j.eurpolymj.2010.07.012

This work describes further investigations into the novel polyaniline (PANI) composite sensors reported previously [13]. The sensors function by the changing of emeraldine polyaniline from its salt form (acidic solutions) to the base form (alkaline solutions). Accompanying the change from salt (ES) to base (EB) is a significant decrease in film conductivity, which arises from the deprotonation of the polymer back bone nitrogen atoms. The sensor response to pH has been described in detail previously [13,15]. In this work, the effect of several film components on the sensor response to pH is investigated. Firstly, the polymer binder, which is used to provide mechanical stability of the film and to bind the film to the underlying substrate is investigated. In a similar set of experiments, the effect of the surfactant (used to prevent particle agglomeration during screen printing) is explored and quantified. Finally, the effect of the sensing layer thickness is examined and the optimum composition of the sensing layer is considered.

2. Experimental

In this work, the sensing layers used are thick films. The screen printing technique was chosen, as it is cost effective, with the added advantages of repeatability and robustness.

Gold thick film conductor pastes (Hereaus Materials) were first screen-printed onto pre-cleaned alumina substrates (CeramTec UK Ltd.) to form an interdigitated electrode (IDE) structure. Gold was chosen as it is an inert material and is commonly used in chemical sensing devices. The deposition of the conductor paste was achieved using a DEK 1202 automatic screen printer. The resulting IDE structures were placed into an oven at 80 °C for 2 h to facilitate the initial drying of the pastes. In this oven the remaining solvent in the paste evaporates, leaving the dried pattern on the substrate. The devices are next placed into a furnace for a much higher temperature (850 °C) cycle. In this step, any remaining organic binder is removed and the metal frit in the paste is sintered into one solid structure. This temperature cycle also allows the electrode pattern to settle to its final thickness and resistivity values.

The thick film paste required for deposition is obtained by mixing the required mass of PANI powder (Sigma–Aldrich – molecular weight >15,000, particle size: 3–100 μm – Product no.: 428329) with 10 wt.% polyvinyl butyral (PVB) (acts as binder), 10 wt.% surfactant (PS3) (stops the agglomeration of polymer particles) and a suitable amount of ethyleneglycolmonobutyalether (solvent). This paste is then screen-printed onto the electrodes as discussed earlier. The device is placed into an oven at 80 °C for 1.5 h to facilitate solvent evaporation. Once out of the oven, link wires can be soldered to the bond pads and the devices are ready for testing. Fig. 1 shows a diagram of the resulting sensor, with the pH-sensitive layer deposited over an IDE structure.

The polymer film thicknesses were measured using a Dektak Surface Profile Measuring System.

The IV characteristics and DC resistance measurements with temperature were carried out using an in house developed IVR profiler, which applies a DC voltage (−14.5 to +14.5 V) and measures the resulting current. The system is also capable of measuring the resistance directly. The measurements can be made at any temperature between 20 and 70 °C. A National Instruments Data Acquisition (DAQ) card controlled by LabWindows/CVI software and driven by customized electronics hardware measured the IV characteristics of the devices.

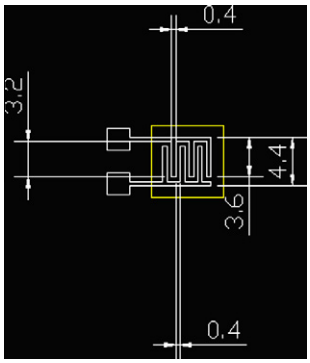

Fig. 1. Conductimetric pH sensor using PANI/PVB/PS3 composite material as the pH-sensitive layer (area outlined by yellow box). All dimensions in the diagram are in mm. (For interpretation of the references in colour in this figure legend, the reader is referred to the web version of this article.)

Testing is carried out by immersing the sensor into 20 ml of test buffer (obtained from Sigma–Aldrich (pH 2–pH 11) – Product no.: 239151) and recording the change in resistance/conductance. The exact pH and temperature of the buffers is measured using a Hanna HI 991001 pH/temperature meter. The changes in electrical parameters of the device are recorded using a HP 4192A Low Frequency Impedance Analyzer and a Thurlby Thandar Instruments Tti 1705 Programmable Multimeter. All AC analysis is undertaken using a 50 mV r.m.s. signal at the required frequency.

SEM images of the resulting films were obtained using a JOEL JSM-840 Scanning Microscope to examine the morphology of the film and to investigate if this changes due to exposure to the test solutions.

XPS analysis was undertaken using a Kratos AXIS 165 spectrometer with a mono Al K_α X-ray source (1486.6 eV) and a base pressure of 9×10^{-10} Torr with a hemispherical analyser. The X-ray source was run at a power of 120 W (10 kV and 12 mA). All binding energies were referenced to the C 1s line of adventitious hydrocarbon peak at 284.6 eV. This analysis was undertaken to observe the changes in the chemical environment of the films due to exposure to solutions of different pH.

3. Results

3.1. Sensing mechanism

From previous work undertaken with PANI composite sensors [13], it was established that the change in the sensing layer conductivity resulted from the protonation/deprotonation of the PANI backbone nitrogen atoms when in contact with a solution. By further exploiting XPS analysis, it was possible to establish the exact nature of the

reaction mechanism. When the sensor is exposed to a buffer solution of know pH value, the protons and hydroxide ions in the solution interact with the PANI in the sensing layer. As the sensing layer is an amorphous film, the solution can penetrate into the layer and interact with the individual PANI particles. The main paths for conduction in such a film arise from particles that are in direct contact with each other, allowing charge carriers to pass easily through the film (ES). When the film comes into contact with an alkaline solution, the particles become insulating (EB) and the conduction paths are significantly reduced. To establish the extent of the deprotonation, an untested ES film was soaked in a pH 10.0 buffer solution for 16 h, rinsed in deionised water and dried thoroughly. The N_{1s} spectrum for the sample was taken and can be seen in Fig. 2(a). Using the inbuilt ion gun on the XPS system, the sample surface was bombarded for several seconds, which removed a portion of the upper particle surfaces. The N_{1s} spectrum was again taken in this region and can be seen in Fig. 2(b).

By comparing the two spectra in Fig. 2, it is clear that the ion-bombardment produced a significant effect on the results obtained. What is evident from the results obtained is that the deprotonation of the sensing layer is a surface effect, and does not affect the bulk of the particle. The spectrum shown in Fig. 2(a) is the common N_{1s} spectrum of PANI EB. After the ion-bombardment, the imine nitrogen intensity is significantly reduced accompanied by an increase in the amine nitrogen signal. This response is a characteristic of the conversion of EB to conducting ES.

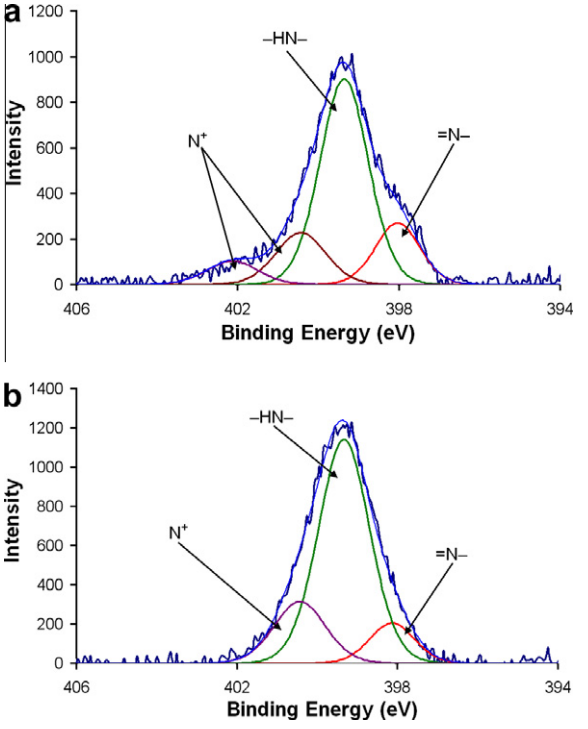

Fig. 2. XPS nitrogen (N_{1s}) spectra of the PANI composite thick film (ES) after 16 h soak in pH 10.0 buffer solution: (a) pre-ion-bombardment; and (b) post bombardment.

If the results in Fig. 2 are compared to the impedance spectra taken of the samples over the entire pH range (frequency range of 10 Hz to 10 MHz), it is possible to fully describe the reactions between the sensing layers and the buffer solutions. The data in Fig. 3(a) shows the electrical characteristics of an untested ES composite film. The equivalent circuit for this data is a simple RC series circuit, with the capacitance component arising from the insulating gaps between the particles. When several samples are soaked for 16 h in different buffer solutions in the pH range 2.0–10.0, there is a significant change in the electrical characteristics. While the acidic solutions do not produce a significant change in the observed film response, i.e. same equivalent circuit (Fig. 3(b)), the imaginary component of the impedance increases significantly when compared to the untested sample (Fig. 3(a)). This result demonstrates

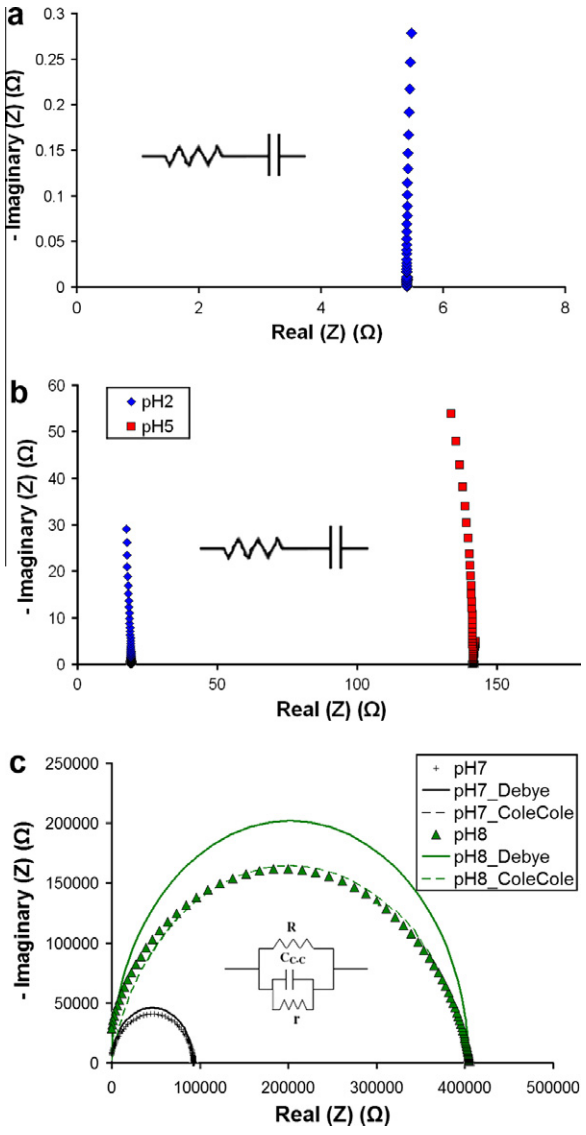

Fig. 3. Impedance spectra of the PANI ES sensing layers (frequency range 10 Hz–10 kHz) showing: (a) untested ES sensing layer; (b) films soaked in acidic solutions; and (c) films soaked in alkaline solutions.

the increasing rate of deprotonation of the outer particle surfaces with increasing pH values. When the test solutions used are alkaline in nature, there is a significant change in the observed sensor response, with an equivalent circuit approximating to a parallel RC arrangement.

It was possible to model the results in Fig. 3 using two models: (1) the Debye model; and (2) the Cole–Cole model [16]. The Cole–Cole model provided the best fit to the data obtained from experiment, and the resulting equivalent circuit was considered. While the initial capacitance term in the untested samples arose from the spaces outside the contact regions of the particles, this has been superseded by the effect of the deprotonated layer. The resistance terms in the circuit arise from the contact regions, where some charge carriers can tunnel through the thin insulating barrier. It is also possible for some ES regions to remain in the insulating layer and thus contribute charge carriers and act as a hopping site for carriers in the bulk of the ES particles. From the information presented in Figs. 2 and 3, it is possible to construct a diagram depicting the nature of the sensing layers after exposure to alkaline solutions. This diagram is presented in Fig. 4.

Unfortunately, the transition between conducting ES and insulating EB does not take place at a well defined pH value, as is suggested by theoretical approaches. If there was a well defined transition, then pH sensing would not be possible using this material. The transition between ES and EB takes place gradually with increasing pH values, and the surface area of the particles are only completely changed to EB at high pH values. Nonetheless, it is still important to understand when the majority of the particle surfaces become EB, as this is the point which the film as a whole becomes semiconducting in nature, rather than metallic as observed for untested films.

According to Talaie [17] the transition between ES and EB occurs between pH 3 and pH 4, while Lindfors and Ivaska [18] gave a much wider range of pH 3–pH 6. Either way it is apparent that the pH-dependent transition occurs in the acidic pH range. To investigate the transition for the purposes of this research, samples were investigated by soaking films in different buffer solutions for 12 h and examining their electrical characteristics. By plotting the log of conductivity against the inverse of temperature, it is simple to distinguish between metallic and semiconducting behaviour, and identify where the transition between the two forms of film conduction takes place. The data in Fig. 5(a) is taken for films soaked in buffers with pH values from 2.0 to 8.0. It can be seen that the transition takes place somewhere between pH 5 and pH 6, which corresponds to the range given by Lindfors and Ivaska [18]. The temperature coefficient of resistance in this case goes from a positive value of 5972.73 ppm/°C at pH 5.0 to a negative value of −8727.27 at pH 6.0, indicating a clear transition. When comparing these results to the diagram in Fig. 4, it can be concluded that, at a pH value greater than 5 and less than 6, the outer surface areas of the particles have become predominantly EB and thus the overall conduction in the film is semiconducting in nature.

By the addition of the correct amount of HCl to the pH 6 buffer solution it was possible to obtain buffers in the pH 5–pH 6 range. This enabled the further investigation of the ES–EB transition pH. By treating the samples in the same way as those in Fig. 5(a), it was possible to

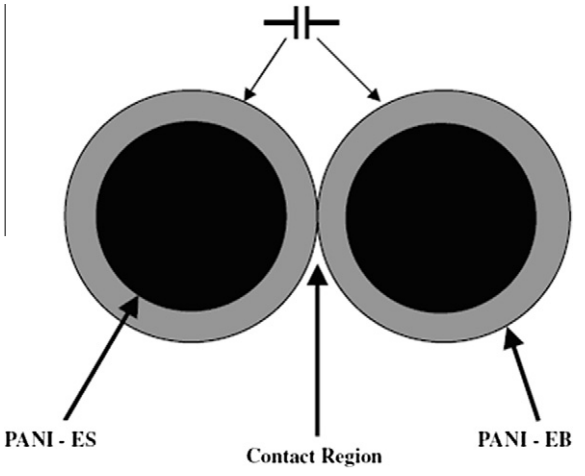

Fig. 4. Diagram showing the nature of two adjacent ES particles after exposure to alkaline buffer solution, in which a thin layer of EB (insulating) forms around the ES and prevents the movement of charge carriers between the particles resulting in an overall reduction in the film conductance.

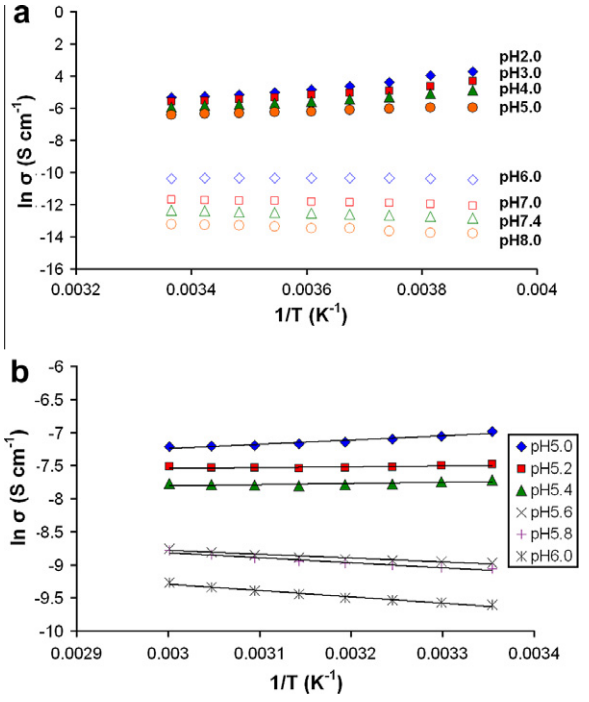

Fig. 5. Log of film conductivity plotted against the inverse of film temperature for samples soaked for 12 h: (a) in buffer solutions in the pH range 2.0–8.0 showing a clear transition from metallic to semiconducting film behaviour between pH 5.0 and pH 6.0; and (b) Log of film conductivity plotted against the inverse of film temperature for samples soaked for 12 h in buffer solutions in the pH range 5.0–6.0 showing a clear transition from metallic to semiconducting film behaviour at approximately pH 5.5.

concentrate on the pH value of interest. Fig. 5(b) shows the temperature dependence of film conductivity in the pH 5–pH 6 region and shows a buffer pH value of approximately 5.5 as the threshold transition pH value. The film parameters, such as TCR and any associated activation energies are summarised in Table 1. As there is now an insulating barrier to be overcome in order for charge carriers to travel through the film, an activation energy can be calculated for each film that has reached the ES–EB transition. The activation energy is obtained from the relationship:

$$\sigma = \sigma_0 \exp\left[\frac{-E_A}{k_B T}\right] \quad (1)$$

The data presented in Table 1 displays the TCR and activation energies (where appropriate) for ES thick films exposed to buffer solutions of known pH values for 12 h. The TCR values of the films decrease steadily from pH 2.0 to pH 5.4, after which the TCR becomes negative and steadily increases in magnitude with increasing pH values. The activation energies also increase with increasing pH values, as was expected from the formation of a more homogeneous EB layer on the surfaces of the ES particles. However, the activation data in Table 1 does not increase steadily with increasing pH. The reason for this is the nature of the buffers used. The pH 5.6, pH 5.8 and pH 6.0 buffers contain extra HCl, resulting in the slightly different activation energies than for the other pH values.

Regardless of apparent differences in activation energies yielded by the different buffer solutions, the values obtained should be approximate values for the activation energy of the EB semiconducting material. According to the results presented by Saravanan et al. [19], the activation energy for their PANI films corresponded to a value of 0.015 eV, which is in the same order of magnitude as that calculated here. The major difference between the samples used by Saravanan and those used here is that the while the samples presented here are deprotonated ES layers, the samples presented by Saravanan et al. are EB films which have been doped with camphor sulphonic acid (CSA). This explains why the activation energies for their films are less than that calculated for the samples presented in this work, as the films here are mostly devoid of charge carriers.

Table 1
Data highlighting the ES film electrical properties after exposure to buffers of known pH values showing the gradual change from metallic to semiconducting conduction over the pH range investigated.

Buffer pH	TCR (ppm/°C)	Activation energy (eV)
2.0	53,499	xxxxx
3.0	31,997	xxxxx
4.0	30,000	xxxxx
5.0	5973	xxxxx
5.2	900	xxxxx
5.4	495	xxxxx
5.6	−5930	0.0493
5.8	−7464	0.0658
6.0	−8727	0.081
7.0	−9008	0.0616
7.4	−9460	0.0788
8.0	−11,111	0.0986

3.2. Effect of polymer binder on sensor characteristics

In screen-printed thick films, the binder is a polymer material that is used to provide adherence between the film and the substrate/electrodes, and also to bind the particles of the functional material together. When there is solvent present (thick film paste) the binder is dissolved while the functional material remains solid. The solid particles are free to move around to some degree. When the particles settle into their final positions, the solvent is removed and the binder solidifies to maintain the particles in these positions. The binder does not coat the particles, as this would restrict the solution penetrating to the functional material and, thus, no sensor response would be observed. It is possible that by adding too much polymer binder to the thick film paste a smaller amount of functional material would be present in the resulting thick film.

The distance between the particles would therefore be much greater than in films with less polymer binder.

For this investigation, different amounts of PVB is added to ES thick films, ranging from 5 to 50 wt.%. In each case the electrical properties of the films are recorded and compared. It was found that the PVB content did not correlate to the change in the film electrical properties. Fig. 6 shows the current–voltage characteristics of the films with different PVB content. While each film displayed an Ohmic relationship between current and voltage, it was found that each film displayed a different resistance value. The film resistance was not proportional to the amount of PVB in the film. With PVB amounts up to 50 wt.%, the conduction mechanism does not vary, suggesting the charge carriers are passing between ES particles in physical contact.

The results in Table 2 show the different TCR and resistance values for the different films. This data supports the results given in Fig. 6, in which it is suggested that there is no apparent correlation between the films with different PVB content. It can be assumed that the resistance of the films, and hence the TCR values are due solely to the arrangement of the ES particles, and not to PVB content, when this content is up to 50 wt.%.

When the films are examined using an A.C. signal, the impedance spectrum for each film can be obtained, as seen in Fig. 3. When the data is plotted, there is no difference observed in the electrical behaviour of the various films.

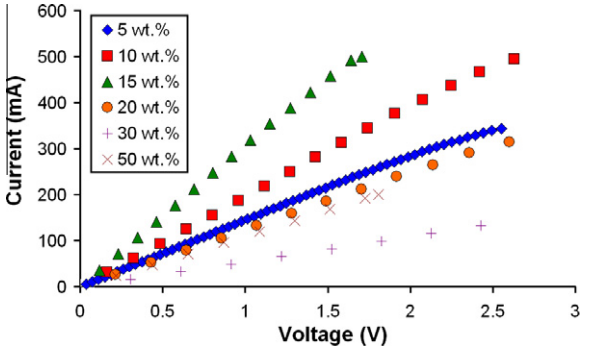

Fig. 6. Current–voltage characteristics of ES thick films containing different amounts (wt.%) of polymer binder (PVB).

Table 2
Electrical properties of ES thick films containing different amounts of PVB polymer binder.

PVB content (wt.%)	TCR (ppm/°C)	R (Ω) (@ 25 °C)
5	5241	9.81
10	3229	5.77
15	3088	3.59
20	4706	11.02
30	5010	20.61
50	2831	9.03

One of the main assumptions of increasing the PVB content was that the distances between the ES particles would increase, leading to a larger capacitive element corresponding to the insulating PVB phase. Fig. 7 shows the impedance spectra for the samples, and, as can be seen, there is no apparent effect of the PVB content on the spectra. Each film possesses the characteristic series RC equivalent circuit behaviour, and there is no obvious increase in the capacitive element.

3.3. Effect of surfactant on sensing mechanism

Another common additive to thick films exploited as the sensing layer in conductimetric pH sensors is a surfactant. In this work, Hypermer PS3 surfactant is used to ensure that the particles of the functional material do not agglomerate to form large clusters. The reason for the use of a surfactant is so large conducting islands are not separated by large insulating phases (polymer binder) thereby reducing the amount of conduction paths through the film. Arshak et al. [20] reported the electrical behaviour of PS3 treated polymer/carbon black films which were used in a gas sensing application. The authors showed how the agglomeration of particles were eliminated by using such a surfactant, and also how this leads to an overall improvement in sensor performance.

The surfactant functions by anchoring itself to the particles in the film and stops the particles from joining together due to electrostatic interaction, as shown in Fig. 8 [20]. By including surfactant in the sensors reported in this work, for both drop coated and screen-printed sensors, the particles were found to distribute themselves more evenly in the film, and an added advantage was the less frequent

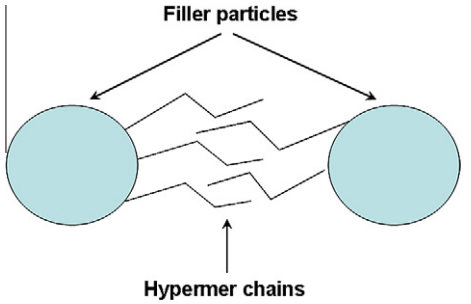

Fig. 8. Mechanism of agglomeration elimination in surfactant treated particles [20].

cleaning required due to particles clogging the pipette or screen.

As only a small amount of surfactant was required to eliminate significant particle agglomeration in the films, it was decided to compare films containing 5 and 10 wt.% PS3 with films containing no surfactant. Much like the results obtained for the investigation into the effects of PVB content of the films, it was found that the characteristics of each of the three film types did not vary due to different PS3 content. In each case the relationship between current and voltage was Ohmic in nature, and when the effects of temperature on the film conductivity was examined, it was observed that there was no change in conduction mechanism due to increased temperature, as seen in Fig. 9. If the surfactant caused the particles to remain a distance apart after the screen printing stage, then there would be some temperature dependent conductivity term, resulting from a hoping conduction between the particles. This would result in a change in the slope of the data in Fig. 9, which was not observed.

Finally, the sensor response for each of the three films was recorded to observe any effect due to the surfactant. Fig. 10 displays the results from this experiment. For the sensors containing no surfactant in the sensing layer, the sensor response is the lowest recorded for ES thick film sensors, with a slope of −0.5023. Even though the particles are compressed into a film during the screen printing process, the absence of surfactant results in some formation of large ES clusters, which in turn results in a decreased sensor sensitivity to pH changes in the test buffers. The main

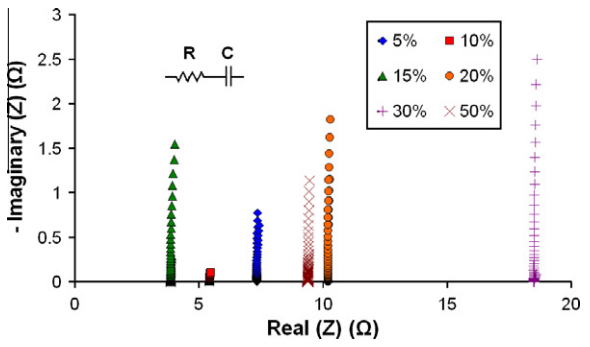

Fig. 7. Impedance spectra for ES thick films containing different amounts of PVB polymer binder.

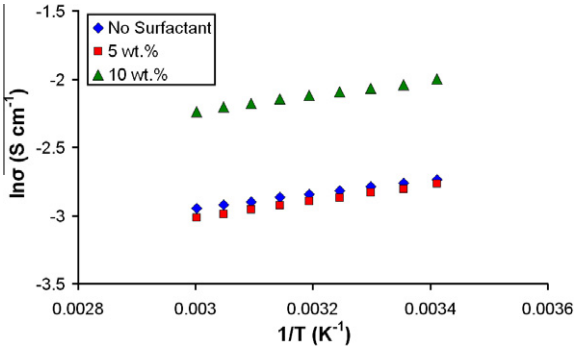

Fig. 9. Effect of surfactant content on the ES thick film electrical properties.

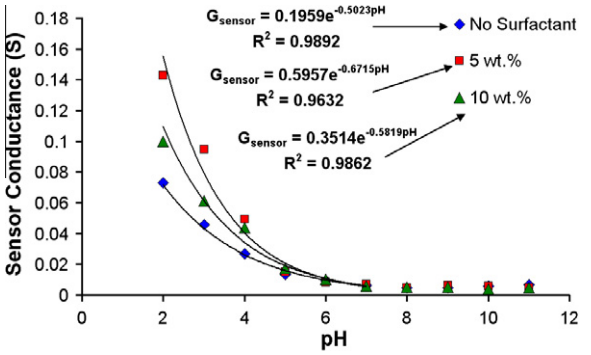

Fig. 10. Comparison of sensor responses for ES thick films containing different amounts of PS3 surfactant.

reason for this is a reduced surface area through which conduction can take place between the ES particles. Although deprotonation is still taking place in the sensing layer, the sensor response is only measurable when this deprotonation occurs around particle contact regions.

For the two sensor batches containing 5 and 10 wt.%, the sensor response is improved when compared to the sensors containing no surfactant. The sensor response in all cases still exhibits an exponential decrease in sensor conductance with increasing pH values, given by Eq. (2):

$$G_{\text{Sensor}} = A\exp[-B\,\text{pH}] \tag{2}$$

where A is the conduction of the film at a buffer pH of 0.0, and B is the slope of the exponential fit, and is also the measured sensor response.

The difference in sensor response for films containing 5 and 10 wt.% is significant. For films containing 5 wt.% PS3, the slope of the exponential fit is −0.6715, while for films with 10 wt.% the response is −0.5819. With the additional surfactant in the 10 wt.% films, the particles are farther apart than those in films with 5 wt.%. However, the fabrication times are greatly increased with the 5 wt.% PS3 films due to more frequent cleaning steps due to particle agglomerate clogging the screen. The response of sensors containing different wt.% of PS3 surfactant is summarised in Table 3.

3.4. Effect of film thickness on sensor response

The final film parameter to be examined is the thickness of the sensing layer. It can be argued that by increasing the film thickness the conductivity of the sensing layer will increase due to the increased amount of conducting functional material, in this case (ES), present. Previous work undertaken by our group investigated a drop coating method for fabricating conductimetric pH sensors [21]. By comparing the thickness of the outer rings in the drop coated sensors to the screen-printed film thicknesses, it can be seen that the resistance does indeed decrease significantly with increasing thickness. Fig. 11 shows the film resistance as a function of film thickness. It can also be seen from the data in Fig. 11 that the deposition method plays an important role in the film conductivity. For drop coated films, the particles tend to pile up on top of the previous layers and depending on the surfactant and binder content, the distance between the adjacent particles can vary. However, by increasing the film thickness, the resistance of the film decreases. For screen-printed films, on the other hand, the particles are compressed together resulting in much more contact between particles, and thus results in a lower film conductivity. If the two films of comparable thickness are compared (one drop coated and one screen-printed), for example the 100 μm drop coated film and the 120 μm screen-printed film, the resistance values of the films are 384.9 and 2.9 Ω, respectively. The differences between the deposition methods results in a nearly three orders of magnitude difference between comparable film resistances, however, for both deposition methods the resistance appears to decrease steadily with increasing film thickness.

Although the film thickness affects the resistance of the film, there is no change in the pH sensitivity of the ES particles. Therefore, it must be assumed that there should be no change in the sensor response of ES based pH sensors due to changes in the sensing layer thickness. Two batches of sensors were used to test this assumption, one with a thickness of 40 μm and the other of thickness 100 μm. Each sensor batch was tested for pH sensitivity and the results are displayed in Fig. 12.

From the data in Fig. 12 it can be clearly seen that the response of both sensors are almost identical. By increasing the thickness of the sensing layer by 250% (40–100 μm) there is a corresponding decrease in sensor sensitivity of 5.62%. If there was an increase in sensor sensitivity, it would be assumed that this would occur by adding more pH-sensitive material to the sensing layer, not by removing it. Therefore, as long as the film over the electrodes is thick enough to

Table 3
Results obtained from ES thick film pH sensors with different amounts of PS3 polymer binder present in the sensing layers.

wt.% PS3	TCR (ppm/°C)	R (Ω) (@ 25 °C)	Sensor response (slope of exponential fit)	R^2 value
0	5829	9.4	−0.5023	0.9892
5	7071	9.82	−0.6715	0.9632
10	6728	4.57	−0.5819	0.9862

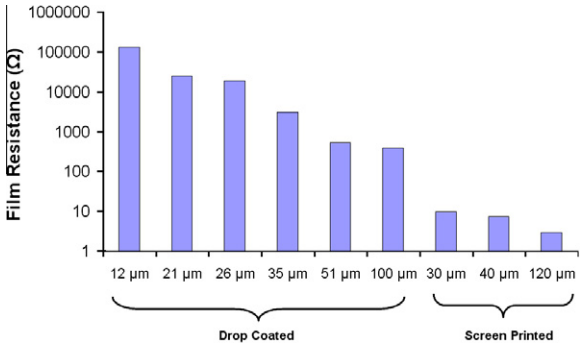

Fig. 11. Resistance of ES thick films as a function of film thickness and deposition method.

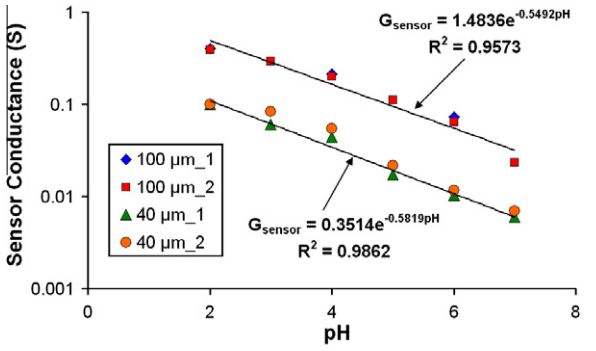

Fig. 12. Sensor response of ES thick film conductimetric pH sensors with two different sensing layer thicknesses.

provide a uniform environment for interaction with the buffer solution, the thickness of this film will not affect the sensor sensitivity by any appreciable amount.

4. Conclusions

This paper described experiments conducted to determine the reaction mechanism in conductimetric pH sensors. By exploiting XPS analysis it was determined that the sensor response is determined by the deprotonation of the PANI ES particles in the sensing layer. The rate of deprotonation increases dramatically with increasing pH values, leading to a pronounced sensor response to pH changes. By using the focussed ion gun (part of Kratos AXIS 165 system) a fraction of the topmost sensing layer was removed to investigate the extent of deprotonation in the bulk PANI material. It was discovered that the deprotonation only takes place on the particle surfaces, and is not a bulk effect. It was thus possible to create a model representing the sensing mechanism of these novel sensors, and use the Cole–Cole model to determine an equivalent circuit at each stage of the deprotonation process.

The effects of polymer binder, surfactant use and film thickness was also investigated in this work to help determine the optimum sensing layer composition. It was found that PVB content up to 50 wt.% had no discernable effects on the electrical characteristics of the sensing layers. It is thought that considerably more PVB is required to affect the average distances between functional particles to change the equivalent circuit behaviour described in Fig. 3(a).

The use of surfactant, unlike the polymer binder, has a significant effect on the response of conductimetric PANI pH sensors. It was observed that when there is no surfactant in the sensing layers, the film conductance is reduced considerably. It is thought that this reduction in film conduction is due to the agglomeration of ES particles, creating large conducting "islands" that are separated by spaces devoid of functional material. By adding 5 wt.% PS3, the film conductance increases and the distribution of ES particles in the film is more homogeneous. By examining the pH response of sensors containing 0, 5 and 10 wt.% PS3, it was discovered that the sensors with the greatest pH sensitivity were those containing 5 wt.% PVB. It is thought that the addition of more than 5 wt.% causes the ES particles to be pushed apart, thereby reducing the particle surface area in contact with its nearest neighbours. Therefore, the conductivity of the films is greatly affected, resulting in a decrease in sensor sensitivity to pH changes.

Finally, the thickness of the films was investigated in terms of the effect this parameter may have on sensor output. Originally, it was thought that the thicker films may provide an improved sensor response, due to the presence of more functional ES material. However, after reviewing the experimental data, it was discovered that there was virtually no difference in the pH sensitivity of sensors with film thicknesses of 40 and 100 μm, respectively. Although the resistance of the 100 μm films was considerably less than the 40 μm films, this was due to the increase in ES particles, which in turn leads to an increase in the number of conducting paths through the film. As the sensor response is dependent on the rate of deprotonation of the ES particles, and not on the number present, this lower film resistance did not directly translate to an increase in sensitivity of the PANI ES conductimetric sensors.

References

[1] Comini E, Faglia G, Sbervegieri G, Alessandri I, Bontempi E, et al. Characterization of P-type Cr:TiO2 gas sensor. Proc IEEE Sensors Conference 2005:1320–2.
[2] Hossein-Babaei F, Keshmiri M, Kakavand M, Troczynski T. A resistive gas sensor based on undoped p-type anatase. Sens Actuators B-Chem 2005;110:28–35.
[3] Wang H, Feng C-D, Sun S-L, Segre CU, Stetter JR. Comparison of conductometric humidity-sensing polymers. Sens Actuators B: Chem 1997;40:211–6.
[4] Wang W, Virkar AV. A conductimetric humidity sensor based on proton conducting perovskite oxides. Sens Actuators B: Chem 2004;98:282–90.
[5] Lee W-Y, Kim S-R, Kim T-H, Lee KS, Shin M-C, Park J-K. Sol–gel-derived thick-film conductometric biosensor for urea determination in serum. Anal Chim Acta 2000;404:195–203.
[6] Arnold FH, Zheng W, Michaels AS. A membrane-moderated conductimetric sensor for the detection and measurement of specific organic solutes in aqueous solutions. J Membr Sci 2000;167:227–39.
[7] Dzyadevich SV, Arkhipova VN, Soldatkin AP, El'skaya AV, Shul'ga AA. Glucose conductometric biosensor with potassium hexacyanoferrate(III) as an oxidizing agent. Anal Chim Acta 1998;374:11–8.
[8] Göpel W, Jones TA, Kleitz M, Lundström J, Seiyama T. Chemical and biochemical sensors. In: Göpel W, Hesse J, Zemel JN, editors. Sensors – a comprehensive survey. New York: VCH; 1991.
[9] Hughes WS. The potential difference between glass and electrolytes in contact with the glass. J Am Chem Soc 1922;44:2860–7.
[10] Kang T-F, Xie Z-Y, Tang H, Shen G-L, Yu R-Q. Potentiometric pH sensors based on chemically modified electrodes with electropolymerized metal–tetraaminophthalocyanine. Talanta 1997;45:291–6.
[11] Sheppard Jr NF, Lesho MJ, McNally P, Francomacaro AS. Microfabricated conductimetric pH sensor. Sens Actuators B: Chem 1995;28:95–102.
[12] Xiaoshan Z, Ahn CH. pH sensor using nano electrodes in organic semiconductor. Engineering in medicine and biology society, 2004. In: IEMBS '04. 26th annual international conference of the IEEE; 2004. p. 1968–71.
[13] Gill E, Arshak A, Arshak K, Korostynska O. pH sensitivity of novel PANI/PVB/PS3 composite films. Sens J 2007;7:3329–46.
[14] Gill E, Arshak K, Arshak A, Korostynska O. Mixed metal oxide films as pH sensing materials. Microsyst Technol 2008;14:499–507.
[15] Gill E, Arshak A, Arshak K, Korostynska O. Investigation of thick film polyaniline-based conductimetric pH sensors for medical applications. IEEE Sens J 2009;9:555–62.
[16] MacDonald JR, Johnson WB. Fundamentals of impedance spectroscopy. In: MacDonald JR, editor. Impedance spectroscopy: emphasizing solid materials and systems. New York: John Wiley and Sons; 1987.

[17] Talaie A. Conducting polymer based pH detector: a new outlook to pH sensing technology. Polymer 1997;38:1145–50.
[18] Lindfors T, Ivaska A. pH sensitivity of polyaniline and its substituted derivatives. J Electroanal Chem 2002;531:43–52.
[19] Saravanan S, Joseph Mathai C, Anantharaman MR, Venkatachalam S, Prabhakaran PV. Investigations on the electrical and structural properties of polyaniline doped with camphor sulphonic acid. J Phys Chem Solids 2006;67:1496–501.
[20] Arshak K, Moore E, Cavanagh L, Harris J, McConigly B, Cunniffe C, et al. Determination of the electrical behaviour of surfactant treated polymer/carbon black composite gas sensors. Compos Part A: Appl Sci Manuf 2005;36:487–91.
[21] Arshak A, Gill E, Arshak K, Korostynska O, Cunniffe C. Drop-coated polyaniline composite conductimetric pH sensors, In: Proceedings of the 30th IEEE ISSE conference. Cluj-Napoca, Romania; 2007. p. 213–8.